IN VITRO STUDY OF BIOFUNCTIONAL INDICATORS AFTER EXPOSURE TO ASBESTOS-LIKE FLUORO-EDENITE FIBRES

A. PUGNALONI [1]✍, G. LUCARINI[1], F. GIANTOMASSI[1], L. LOMBARDO[2], S. CAPELLA[3], E. BELLUSO[3,4], A. ZIZZI[1], A.M. PANICO[2], G. BIAGINI[1] AND V. CARDILE[2]

[1]✍Dipartimento di Patologia Molecolare e Terapie Innovative - Istologia, Università Politecnica delle Marche, Via Tronto 10/A, 60020, Torrette, Ancona, Italy, Fax +39.071.2206.073; e-mail: armanda.pugnaloni@univpm.it
[2]Dipartimento Scienze Fisiologiche, Università degli Studi di Catania, Viale A. Doria 6, 95125 Catania Italy.
[3]Dipartimento di Scienze Mineralogiche e Petrologiche, Università degli Studi di Torino, Via Valperga Caluso 35, 10125 Torino, Italy.
[4]CNR Istituto di Geoscienze e Georisorse – Sezione di Torino, Via Valperga Caluso 35, 10125 Torino, Italy.

Abstract – The *in vitro* biological response to fluoro-edenite (FE) fibres, an asbestos-like amphibole, was evaluated in lung alveolar epithelial A549, mesothelial MeT-5A and monocyte-macrophage J774 cell lines. The mineral has been found in the vicinity of the town of Biancavilla (Catania, Sicily), where an abnormal incidence of mesothelioma has been documented. Cell motility, distribution of polymerized actin, and synthesis of vascular endothelial growth factor (VEGF) and of ß-catenin, critical parameters for tumour development, progression and survival, were investigated in A549 and MeT-5A cells exposed to 50 µg/ml FE fibres for 24 hr and 48 hr. The levels of cyclooxygenase (COX-2) and prostaglandin (PGE$_2$), two molecules involved in cancer pathogenesis by affecting mitogenesis, cell adhesion, immune surveillance and apoptosis, were measured in J774 cells treated with FE fibres under the same experimental conditions. Finally, FE fibres were studied by SEM and EDS analysis to investigate their chemical composition. Exposure of A549 and MeT-5A cells to FE fibres affected differentially phalloidin-stained cytoplasmic F-actin networks, cell motility and VEGF and β-catenin expression according to the different sensitivity of the two cell lines. In J774 cells it induced a significant increase in COX-2 expression, as assessed by Western blot analysis, and in the concentration of PGE$_2$, measured in culture media by ELISA. SEM-EDS investigations demonstrated two types of FE fibres, edenite and fluoro-edenite, differing in chemical composition and both recognizable as calcic amphiboles. Fibre width ranged from less than 1 µm (prevalently 0.5 µm) to 2-3 µm (edenite) up to several µm (fluoro-edenite); length ranged from about 6 to 80 µm (edenite) up to some hundred µm (fluoro-edenite). Results provide convincing evidence that FE fibres are capable of inducing *in vitro* functional modifications in a number of parameters with crucial roles in cancer development and progression. Inhaled FE fibres have the potential to induce mesothelioma, even though their ability to penetrate lung alveoli depends on their aerodynamic diameter.

Key words: Amphibole fibres, Fluoro-edenite, Lung cancer, Cell transformation, In vitro culture, VEGF, ß-catenin, F-actin.

INTRODUCTION

The abnormal incidence of pleural mesothelioma recorded among the inhabitants of Biancavilla (Catania, eastern Sicily, Italy) has recently been linked to environmental exposure to respirable mineral fibres. However, none of

Abbreviations: CNMMN, Commission on New Minerals and Mineral Names; **COX-2,** cyclooxygenase-2**; EDS,** energy dispersive X-ray spectroscopy; **FE,** fluoro-edenite; **MTT,**3-(4,5-dimethylthiazol-2-yl)-2.5 diphenyltetrazolium-bromide test; **PG2,** prostaglandins E$_2$**; ROS,** reactive oxygen species; **SEM,** scanning electron microscope; **VEGF,** vascular endothelial growth factor**.**

the residents of Biancavilla diagnosed with the disease had been occupationally exposed to mineral fibres. A possible cause was discovered in the course of a periodic epidemiological surveillance programme, conducted in every Italian municipality by the Italian Istituto Superiore di Sanità, in the material extracted from the local quarries found on M. Calvario, on the south-western side of the Etna volcano (27). The stone, used locally as building material until a few years ago, contains large quantities of fluoro-edenite (FE), an amphibole with a prismatic, acircular fibrous habit similar to that of amphibole asbestos. The high incidence of malignant mesothelioma in the area of Biancavilla was ascribed to breathing airborne

fibrous FE from building materials, as in occupational exposure to asbestos (26). Mesothelioma is relatively infrequent compared to other tumours, such as breast, prostate, colorectal and renal cell carcinoma, but carries a poor prognosis and is considered an asbestos-related condition (4, 17, 18, 33).

Recently, the Commission on New Minerals and Mineral Names (CNMMN) has recognized FE as a new edenite end-member (17). To date, its correlation with tumour processes has been explored in a small number of epidemiological, experimental and *in vitro* studies (33). The poor outcome of malignant mesothelioma could be related, among other factors, to a) the difficulty in characterizing cell markers for neoplastic transformation after asbestos exposure, and b) the uncertainty as to which asbestos species poses the highest risk, albeit crocidolite currently appears to be the most dangerous (4, 19, 24). Further information on FE is thus required, on the salient aspects of its toxicity and its role in neoplastic cell transformation.

There is a well-established functional relationship between inflammation and cancer (1, 28), with cancer frequently arising in areas of chronic inflammation. Inflammatory cells can promote cancer by secreting cytokines and growth factors that stimulate epithelial proliferation and generate oxygen free radicals (ROS), which can cause DNA damage (4, 25). Epithelial cells are also involved in this inflammatory cross-talk through autocrine production of growth factors and a redistribution of cytoskeletal molecules that result in impaired intercellular relationships in tissues. Cell culture experiments are therefore still essential to studying specific cell steps in the malignant transformation of lung cells.

Recent *in vitro* investigations show that FE induces marked tropism, cell cycle perturbation and increased release of proinflammatory IL-6 cytokines in alveolar epithelial A549 cells (33).

For the present study we used A549, MeT-5A and J774 cells (respectively human pulmonary type II-like epithelial cancer, human pleural mesothelial and mouse monocyte-macrophage cell lines), which are commonly used to assess the degree of cytotoxicity of various silica dusts (14). Epithelial cells are involved in proinflammatory effects and are the cells of origin of bronchogenic carcinoma; they can thus be used to test both end points.

Mesothelial cells are cells whose transformation leads to mesothelioma, so they are suitable for determining the direct effects of fibres. Alveolar macrophages are the first defence mechanism against particles and fibres entering the lower respiratory tract. Their interaction with the fibres results in generation of oxidants, inflammatory cytokines and growth factors that are believed to play critical roles in fibre-induced diseases. The cell lines used in *in vitro* studies (14) usually derive from human lung tumours (e.g. A549 cells), from spontaneously immortalized cells, or from cells transfected with viral oncoproteins (e.g., MeT-5A), which may alter their genotoxic, apoptotic, or proliferative responses.

Given that tumour development and progression are largely dependent on cell motility, we investigated the distribution of polymerized actin in A549 and MeT-5A cells exposed to FE fibres (7). In these same cells we tested the effect of FE exposure on the synthesis of vascular endothelial growth factor (VEGF) and ß-catenin, two critical steps of epithelial cell activation pathways. VEGF has an important role because blood vessels are critical for tumour survival: without new blood vessels a carcinoma cannot grow beyond a very small size, nor can it metastasize to distant organs (5). The action of ß-catenin is another significant step in neoplastic transformation, since activation of the Wnt-ß-catenin pathway is a signalling cascade closely involved in the activation of transcription processes during cancer development (3).

We also investigated the expression of cyclooxygenase (COX-2) and prostaglandin (PGE$_2$) levels in FE-exposed J774 monocyte-macrophage cells. Alveolar macrophages play a critical role in the fibrotic process involved in silicosis and in several other lung diseases (32). They are key mediators in the interaction between inhaled particulate and various cell types, e.g. lymphocytes and fibroblasts, by the release of a variety of inflammatory and growth-mediating factors, as well as cytokines (21). COX-2, an enzyme that catalyses the conversion of arachidonic acid to prostaglandins (PGs), is mainly induced in response to proinflammatory stimuli, cytokines, growth factors and mitogens. The enzyme is upregulated in several human tumours associated with increased production of PGs, which have a large role in cancer pathogenesis since they affect mitogenesis, cell adhesion, immune surveillance and apoptosis. Products of arachidonic acid metabolism are thus critical participants in the development of

inflammatory responses after infection or tissue injury. Prostaglandin E_2 (PGE_2) is one of the most thoroughly studied mediators of this process (13).

Finally, the chemical components of the FE fibres used in the tests were studied by SEM and EDS analysis.

MATERIALS AND METHODS

Fibre characterization

Mineral fibres from a quarry on M. Calvario (provided by A.M. Panico and V. Cardile) were studied using a Cambridge Stereoscan 360 (UK) scanning electron microscope (SEM) equipped with an EDS microprobe (INCA 2000 Oxford Instrument, UK). After careful manual separation from impurities under the light microscope, to avoid any reduction in size, fibres were glued onto an aluminium pin stub using a conductive double-sided adhesive, and coated with a carbon film approximately 400 Å in thickness. A polished sample to obtain quantitative chemical data could nor be prepared owing to their small size (diameter < 1.5 μm).

Secondary and backscattered electron images were obtained from several fibres in order to define morphological and size characteristics. Several X-ray dispersive energy spectra were obtained from different fibres in view of their chemical characterization and identification.

Cell cultures and treatments

We used A549 (human alveolar epithelial cancer), MeT-5A (human mesothelial) and J774 (mouse monocyte-macrophage) continuous cell lines, which are widely employed in toxicological tests of mineral fibres, to test a number of biological responses to FE (8, 15, 29).

A549 cells (kindly donated by D. Ghigo, Dipartimento di Genetica, Biologia e Biochimica, Università di Torino) were grown in controlled atmosphere (5% CO_2; T=37°C) in DMEM (Sigma, Milan, Italy) supplemented with 10% foetal bovine serum (FBS), 1% non-essential amino acids, 2.0 mM L-glutamine, and antibiotics. Cells were routinely split 1:2 each week and used between the 4th and 5th passage. Cells from confluent cultures were detached with 0.25% trypsin–1 mM EDTA and seeded in DMEM medium.

MeT-5A cells (obtained from American Type Culture Collection, Rockville, MD, USA) were grown in RPMI medium in the same culture conditions as A549 cells.

J774 cells (also obtained from American Type Culture Collection) were cultured in DMEM containing 10% foetal calf serum, 4.5 g/L glucose, 1 mM sodium pyruvate, 100 U/ml penicillin, 100 μg/ml streptomycin, and 25 μg/ml fungizone (Invitrogen, UK) and incubated in 5% CO_2 at 37°C. The medium was changed every three days and subcultures were performed every 8-10 days.

FE exposure was by addition of 50 μg/ml fibres to culture media for 24 and 48 hr before cell harvesting (33).

Controls were the three cell lines cultured without fibres for 24 and 48 hr.

Cell viability

The MTT [3-(4,5-dimethylthiazol-2-yl)-2,5-diphenyl tetrazolium bromide] colorimetric assay was performed to assess cell viability through mitochondrial succinate dehydrogenase enzyme activity.

Cells seeded in 24–well plates at a density of $3.5x10^4$cells/cm^2 in DMEM were exposed to FE a few hours after seeding, in order to favour adhesion to the substrate, by 24 and 48 hr incubation with the fibres (50 μg/ml medium). The medium was then removed. Subsequently, 200 μl MTT (Sigma-Aldrich 135038, St. Louis, MO) solution (5 mg/ml in DMEM, without phenol red) and 1.8 ml DMEM were added to the cell monolayer, and the plates were further incubated at 37°C for 3 hr. After discarding the supernatants, the dark blue formazan crystals were dissolved by adding 2 ml of solvent (4% HCl 1N in absolute isopropanol) and quantified spectrophotometrically (Secomam, Anthelie light, version 3.8, Contardi, Italy) at 570 nm. Means and standard deviations (SD) were obtained from three different experiments.

Time-Lapse Microscopy

For time-lapse videomicroscopy, A549 and MeT-5A cells were seeded in 24-well plates at a density of $1x10^4$cells/cm^2 in DMEM and RPM1 respectively, supplemented with 10% FBS. Cells were treated a few hours after seeding, in order to favour substrate adhesion, by 24 and 48 hr incubation with 50 μg FE/ml medium. Subsequently, fibres were removed by several washes in PBS and cells incubated in Hepes-modified DMEM or RPM1 supplemented with 10% FBS, 2 mM L-glutamine, 100 U/ml penicillin, and 100 U/ml streptomycin. For time-lapse recordings, cells were maintained at 37°C and observed under an Eclipse TS-100 inverted microscope (Nikon, Japan) equipped with a x 10 objective and a colour CCD video camera (JVC TK9 C1381, Japan). Phase-contrast images of living cells were recorded using an AG-TL700 time-lapse VCR (Panasonic, Japan) and digitalized using a video frame grabber card and live cell-dedicated software (Image - Pro Express, Media Cybernetics Inc., MD, USA). The same culture fields were filmed by capturing images every 10 min for up to 24 hr to record cell movement during migration phases. The motion of 10 selected cells in a selected microscope field was recorded and plotted. Unattached, round cells and cells dividing during recording intervals were not considered. Diagrams of cell displacement were obtained by processing data with Microsoft Excel, plotting them as x-y diagrams and expressing them as pixel tracks. Migrating cells produced linear tracks, whereas immotile cells were associated with spot-like pixel sequences. Plots were representative of standardized spatial changes in time.

F-actin staining

Fluorescent phalloidin staining was performed to localize cytoskeletal filamentous actin.
A549 and MeT-5A cells were seeded onto two-glass chamber slides at a density of $3.5x10^4$cells/cm^2 in DMEM. Cells were treated with 50 μg FE /ml medium when near to confluence and incubated for 24 hr and 48 hr. They were then washed in PBS, fixed in 4% formaldehyde solution in PBS for 15 min at 37°C and permeabilized in 0.5% Triton X-100 buffer for 15 min. After an incubation in bovine serum albumin/PBS at 37°C, an FITC-conjugated phalloidin solution (1:200 dilution in PBS) was added for 30 min at 37°C. Phalloidin was then removed by washing in PBS and samples were examined using a Nikon Eclipse E 600 fluorescence microscope.

Immunohistochemistry

Cell monolayers were fixed in cold acetone for 10 min, permeabilized in 0.1% Triton X-100 in PBS for 10 min and incubated overnight at 4°C with anti-VEGF (1:200 dilution) and anti-β-catenin (1:100 dilution) monoclonal antibodies (both from Santa Cruz, CA, USA). Cells were then immunostained using the streptavidin-biotin peroxidase technique (LSAB peroxidase kit, Dako Cytomation, Milan, Italy). After incubation with 3.3'-diaminobenzidine (0.05 diaminobenzidine in 0.05 M Tris buffer, pH 7.6 and 0.01% hydrogen peroxide), sections were counterstained with Mayer's haematoxylin and coverslipped with mounting medium. Immunohistochemical VEGF and β-catenin expression was evaluated by light microscopy. Stained cells were counted under the light microscope in about 10 fields/sample at x 200 magnification. Positive cells were expressed as a proportion of counted cells.

Staining intensity was assessed using a four-point scoring system: +- = slight staining, + = weak focal staining; ++ = moderate staining; +++ = strong staining (31). Counts were performed simultaneously by two investigators who used a double-headed light microscope and had to agree on the count of positive cells.

Each experiment was performed three times in quadruplicate; the mean ± SD was considered for each value. All results are expressed as mean ± SD. Differences between groups were analysed using Student's t-test.

Western blot analysis

Expression of COX-2 was evaluated in control and FE-treated J774 cells by Western blot analysis. Briefly, harvested cultures were washed twice with ice-cold PBS, collected with lysing buffer (50 mM Tris-HCl pH 7.5 plus 20 mM EDTA and 0.5% SDS); after 30 min on ice, they were homogenized and centrifuged at 13,000 x g for 15 min. Twenty micrograms of total protein from the surnatant was loaded per lane and separated by 10% Novex Bis-Tris gel electrophoresis (NuPAGE, Invitrogen) as described by Laemnli (22). The separated proteins were then transferred to nitrocellulose membranes (Invitrogen) in a wet system. Protein transfer was verified by staining the nitrocellulose membranes with Ponceau S and the Novex Bis-Tris gel with Brillant blue R. Membranes were blocked in Tris-buffered saline containing 0.01% Tween-20 (TBST) and 10% non-fat dry milk at 4°C overnight. Primary mouse monoclonal COX-2 antibody (Cayman Chemical, Ann Arbor, MI, USA) and rabbit polyclonal β-tubulin antibody (Sigma) were diluted 1:1000 in TBST and incubated for 2 hr at room temperature. Antibodies were detected with horseradish peroxidase-conjugated secondary antibody using the enhanced chemiluminescence detection Supersignal West Pico Chemiluminescent Substrate (Pierce, Rockford, IL, USA). Bands were measured densitometrically; their relative density was calculated based on the density of the α-tubulin band in each sample. Values were expressed as arbitrary Densitometric Units (D.U.) corresponding to signal intensity.

PGE$_2$ determination

The concentration of PGE$_2$ was measured in culture media by enzyme-linked immunosorbent assay (ELISA) (Kit Biotrak PGE$_2$ Amersham Pharmacia Biotech, UK) according to the manufacturer's instructions. Briefly, 50 μl of surnatant was dispensed into a 96-well microplate to which 50 μl of diluted antibody and 50 μl of diluted conjugate were added. After incubation at room temperature for 1 hr, wells were washed 4 times with wash buffer followed by 150 μl of room temperature-equilibrated

enzyme substrate. The plate was mixed on a microtitre plate shaker for 30 min at room temperature. The reaction was stopped by adding 100 μl of 1 M sulphuric acid to each well. Sample optical density was measured with a microplate spectrophotometer reader (Titertek Multiskan, Flow Laboratories, McLean, VA, USA) at $\lambda_.$ = 450 nm within 30 min.

Each experiment was repeated at least three times in triplicate and the mean ± SD was calculated for each value. Statistical analysis of results was performed using Student's t-test and one-way ANOVA by the statistical software package SYSTAT, version 9 (Systat Inc., Evanston IL, USA). A difference was considered significant at P < 0.01.

RESULTS

Fibre characterization

SEM showed only fibre bundles (Fig. 1). Fibres were closely associated and parallel to the fibre axis; they revealed two types of chemical composition (a and b), both recognizable as calcic amphiboles. The EDS spectra in Figure 2 show the elemental composition of edenite (Fig. 2 a) and fluoro-edenite (Fig. 2 b).

Width varied from less than 1 μm (mostly 0.5 μm) for both fibres to 2-3 μm for (a) fibres up to many μm for (b) fibres. These are the original fibre dimensions, since any manipulation, even with tweezers, caused a decrease in size, especially in width, due to longitudinal parting. This also occurs in natural conditions, as fibres contained in outcropping rocks gradually become exposed due to weathering or to erosion caused by human activity, like erionite fibres in central Turkey (15).

The relative amount of the two fibre species varied between bundles. Their length ranged from ~ 6 to 80 μm for edenite and to some hundred μm for fluoro-edenite.

Cell viability

Control culture absorbance was 0.201 ± 0.007 (A549 cells) and 0.094 ± 0.013 (MeT-5A cells) at 24 hr, and 0.764 ± 0.031 and 0.119 ± 0.015 at 48 hr. These values were considered as 100% of cell viability (Fig. 3).

Incubation with FE for 24 hr yielded values of 0.170 ± 0.008 (or 84.57% of control values) in A549 cells and of 0.073 ± 0.013 (77.66%) in MeT-5A cells. At 24 hr cell viability was thus still quite high in both cell lines.

Absorbance at 48 hr was 0.559 ± 0.016 (73.16%) in A549 cells and 0.075 ± 0.010 (63.02%) in MeT-5A cells. At 48 hr cell viability was further decreased, but still partially preserved.
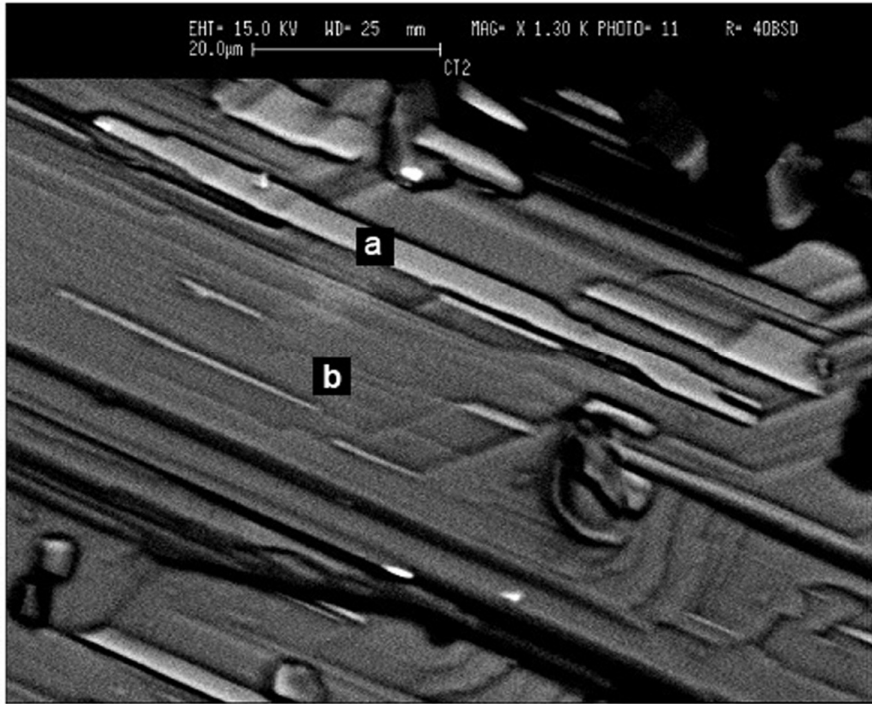
Figure 1. Backscattered electron SEM image of fibre intergrowth of the two amphibole species. Dark fibrous lamellae (b) with the chemical composition of fluoro-edenite are larger and more numerous than light fibres (a), chemically corresponding to the edenite phase.
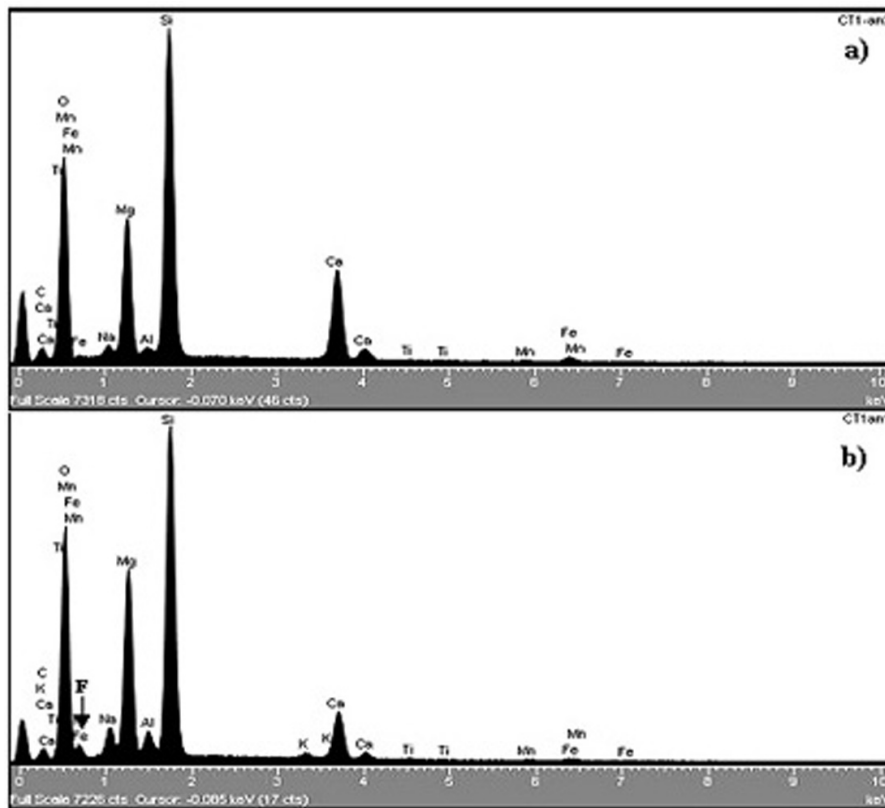
Figure 2. EDS spectra of a) edenite and b) fluoro-edenite fibres. Different peak Mg and Ca height ratios compared to Si allows to distinguish the two minerals, with F being found only in b).
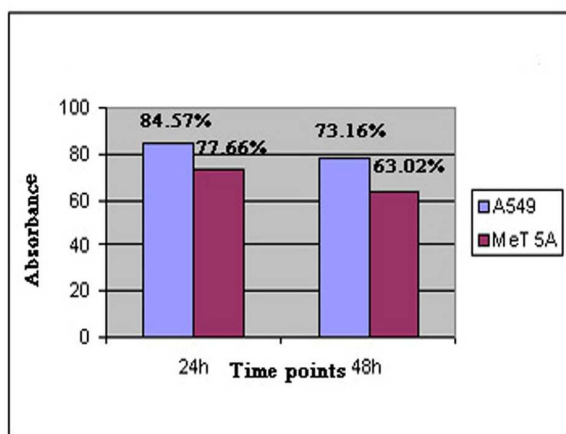
Figure 3. Effects of FE treatment on A549 and MeT-5A cell viability determined by the MTT colorimetric assay (testing mitochondrial succinate dehydrogenase activity). Absorbance values of control and treated cell lines at 24 hr and 48 hr are mean ± SD of at least three different experiments. Control cell absorbance values were taken as 100% of cell viability. Treated cultures at 24 hr and 48 hr show lower though still moderate absorbance reductions compared with control cultures.

Time-Lapse Microscopy

Figure 4 shows cell displacements plotted on x-y diagrams. Since cell density in microscopic fields was lower in treated cultures, due to the action of the fibres, cell motility was monitored only in 5 cells.

At 24 hr motility was greater in treated A549 cultures (Fig. 4 c) than in control A549 cells (Fig. 4 a), as shown by longer linear tracks, whereas it was diminished at 48 hr, as reflected by shorter (spot-like) tracks related to reduced spatial motion (Fig. 4 e). Similarly, cell motion in treated MeT-5A cells was considerably reduced at 24 and 48 hr (Fig. 4 d and f) compared with control MeT-5A cultures (Fig. 4 b).

Overall, cell movement was greater in control MeT-5A (Fig. 4 b) than in control A549 cells; however, movement of MeT-5A ceased after 24 hr incubation with FE (Fig. 4 d and f), as shown by punctiform tracks.

F-actin staining

Phalloidin staining of F-actin at 24 hr had a more granular appearance in treated A549 and MeT-5A cells (Fig. 5 b, d) than in the respective control cultures. In A549 cells, a tumour cell line, expression of actin fluorescence in the control culture (Fig. 5 a) was good at both time points and was more homogeneously distributed in the cytoplasm than in control MeT-5A cells, a non-tumour cell line (Fig. 5 c). In the latter cells,

phalloidin cell staining was not uniform. In treated MeT-5A cells actin staining was more irregular in the cytoplasm and more granular than in the respective control cultures, also at the level of the plasma membrane, suggesting altered actin polymerization dynamics. Granular fluorescence was also detected in treated MeT-5A cells (Fig. 5 d), thus confirming that actin does not assemble correctly in the presence of FE.

Immunohistochemistry

VEGF and ß-catenin expression in control and FE-exposed A549 cells at 24 and 48 hr (Fig. 6; Tab. 1).

At 24 hr an increased number of treated cells expressed VEGF and ß-catenin, and the intensity of staining with the two markers was increased both in the cytoplasm and in the peripheral membranous protrusions. At 48 hr treated cells exhibited only an increased intensity of ß-catenin cytoplasmic expression.

24 hr (Fig. 6 a-d). At this time point, control cells displayed moderate VEGF expression both in perinuclear zones and in cytoplasmic extensions (Fig. 6 a). Treated cells exhibited more intense and diffuse cytoplasmic staining and a significantly greater number of positive cells than control cultures (p= 0.002), (Fig. 6 b).

In control cultures expression of anti ß-catenin antibody was focal, especially at intercellular contacts at the level of the plasma membrane. Irregular positivity was also observed in the cytoplasm (Fig. 6 c). β-catenin-positive cells were significantly increased in treated cultures (p=0.002) (Fig. 6 d) compared with control cells, with staining being prevalently noted at intercellular contacts. Focal cytoplasmic positivity was also detected.

48 hr (Fig. 6 e-h). At this time point, control cells exhibited moderate VEGF positivity, mainly at the perinuclear level (Fig. 6 e). Sparse dead cells were also detected. In FE-treated cells, positivity for VEGF was similar in intensity, localization (Fig. 6 f) and number of positive cells. Scattered dead elements were also observed.

In control cultures expression of ß-catenin was strong on the membrane at intercellular contacts (Fig. 6 g), while the cytoplasm was faintly positive. The pattern was similar in treated and control cells, but staining was slightly stronger in the cytoplasm of FE-exposed cells (Fig. 6 h).
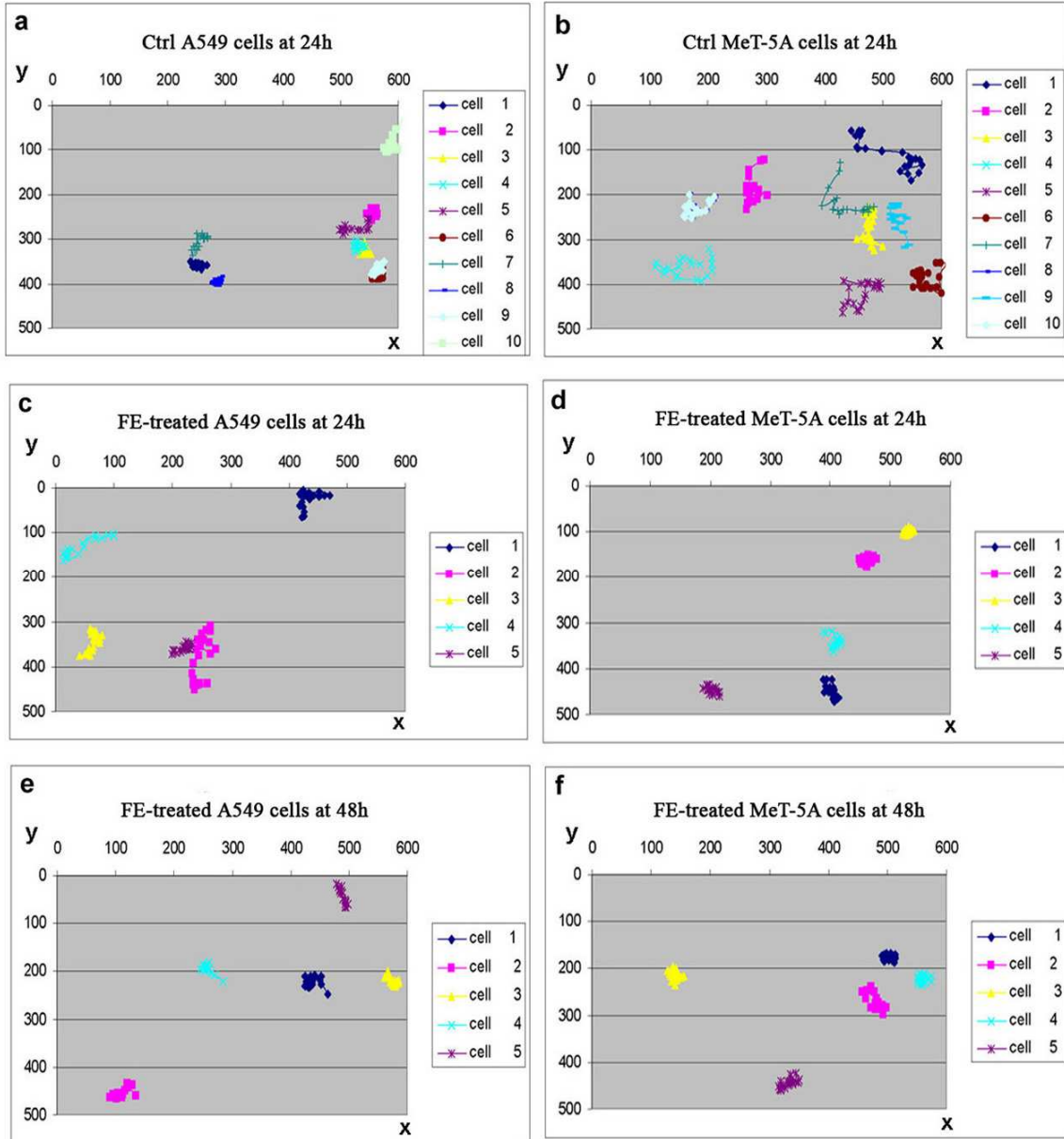
Figure 4. Time-lapse videomicroscopy recordings of A549 and MeT-5A cell line motility in control (a-b) and FE-exposed (c-f) cultures at 24 hr and 48 hr. x-y plots of cell movements recorded by time-lapse video microscopy. In FE-treated cultures only 5 representative cells were considered because of the lower cell density in these cultures in equivalent areas, due to cell loss after fibre exposure.
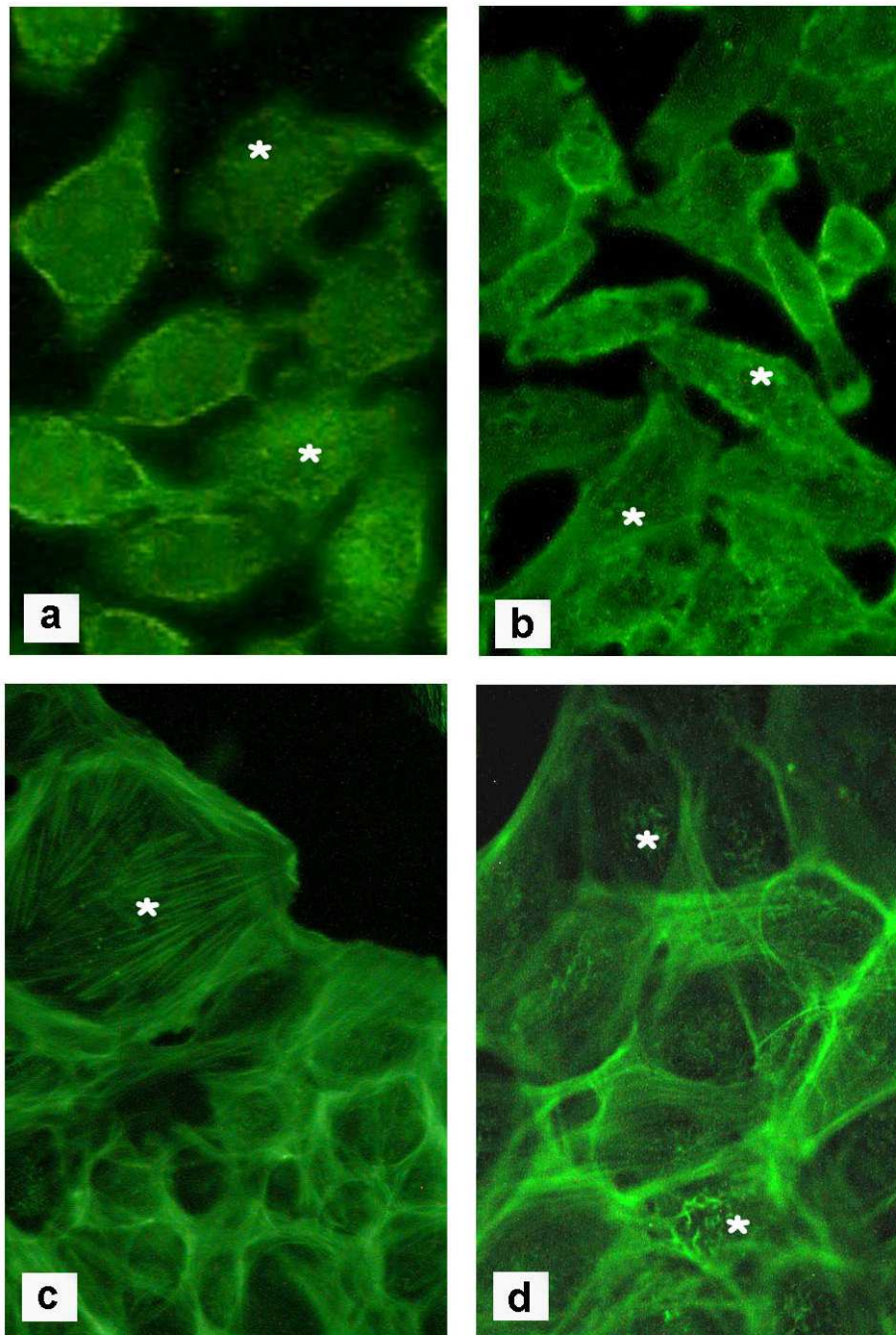
Figure 5 (a-d). Fluorescence imaging of phalloidin staining for F-actin detection in A549 and MeT-5A cells at 24 hr (x 400 original magnification). (a) Control A549 cell cultures: diffuse cytoplasm and membrane phalloidin staining (*); (b) FE-treated A549 cells: treatment induced a more irregular and granular phalloidin staining (*) of F-actin compared with control cultures (a); (c) Control MeT-5A cell cultures: phalloidin staining (*); (d) FE-treated MeT-5A cells: phalloidin staining of F-actin (*) has a more granular appearance than in control cultures (c).

Table 1. VEGF and ß-catenin expression in control and FE-treated A549 and Met-5A cells at 24 and 48 hr.

24 hr	VEGF			ß-catenin		
	Percentage of positive cells (± SD)	Staining intensity in cytoplasm	Staining intensity in extensions	Percentage of positive cells (± SD)	Staining intensity in cytoplasm	Staining intensity in plasma membrane
A549 Ctrl	50±1.20	+	+	25±8.0	+-	+
A549 FE	70±10.15	++	++	50±10.0	+	++
MeT-5A Ctrl	50±3.25	+-	+-	90±12.10	+/++	+/++
MeT-5A FE	60±12.10	+	+	85±5.0	++/+++	++
48 hr						
A549 Ctrl	85±13.10	+	+-	75±1.0	+-	++
A549 FE	87±8.50	+	+-	70±3.5	+	++
MeT-5A Ctrl	35±5.0	+-/+	+-	40±2.0	+	+-
MeT-5A FE	50±7.10	+	+-	60±7.0	+/++	+-

Ctrl: control culture; FE: FE-treated culture.
+-: slight staining; +: focal and weak staining; ++: moderate staining; +++: strong staining.
Values are expressed as the percentage of total counted cells ± SD.

Statistical analysis (Student's t-test):

VEGF+ A549 Ctrl 24 hr   vs   VEGF+ A549 FE 24 hr: p=0.002

β-catenin+ A549 Ctrl 24 hr   vs   β-catenin+ A549 FE 24 hr: p=0.002

VEGF+ MeT-5A Ctrl 48 hr   vs   VEGF+ MeT-5A FE 48 hr: p=0.005

β-catenin+ MeT-5A Ctrl 48 hr vs   β-catenin+ MeT-5A FE 48 hr: p= 0.000
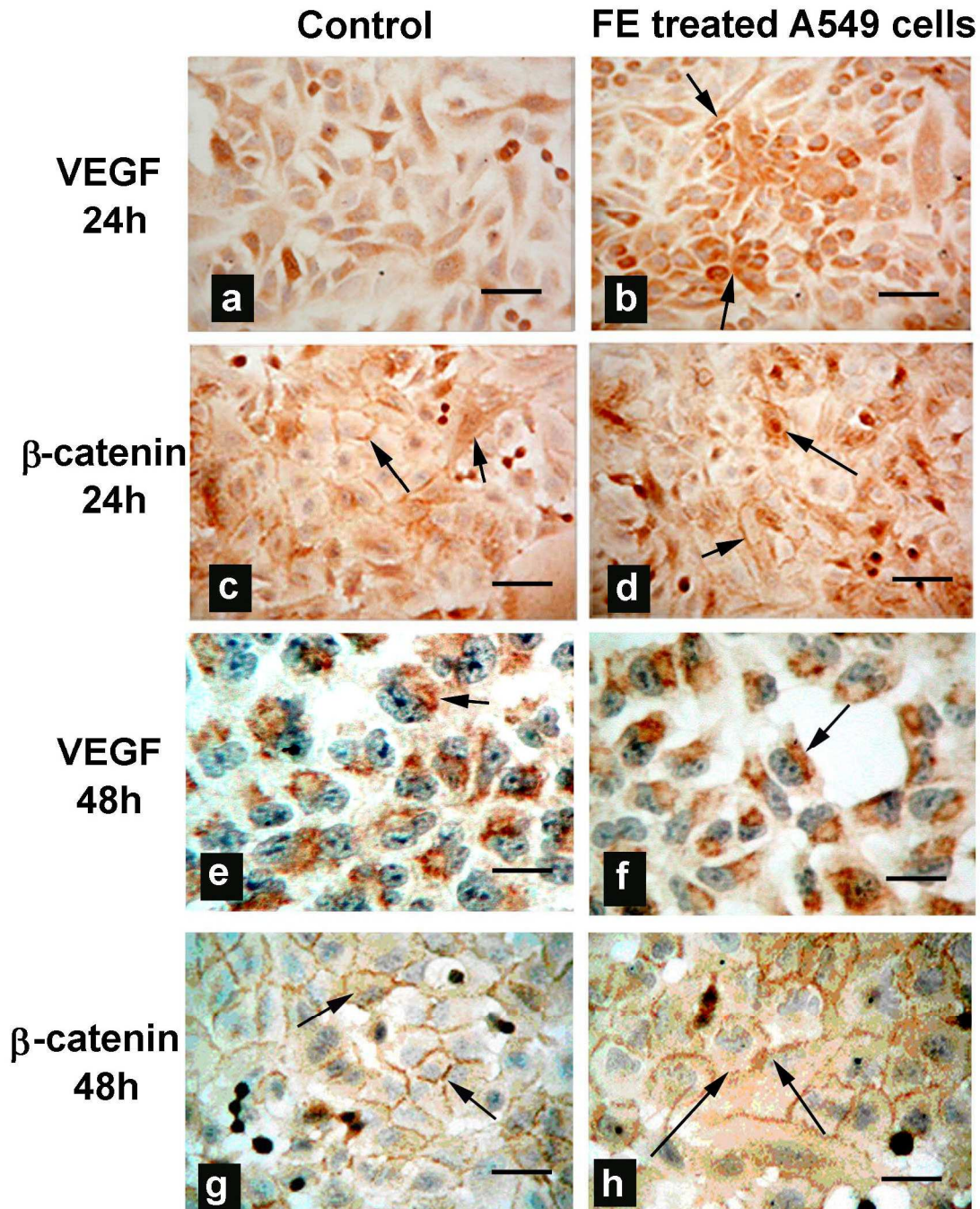
Figure 6 (a-h). VEGF and ß-catenin expression in control and FE-treated A549 cell cultures at 24 hr (a-d) and 48 hr (e-h). (immunoperoxidase). (a) Control A549 cell cultures at 24 hr: moderate VEGF expression (arrows) both in perinuclear zones and in cytoplasmic extensions (bar = 35µm); (b) FE-treated A549 cell cultures at 24 hr: stronger VEGF expression with broad cytoplasmic diffusion (arrows) compared with control A549 cells (a) (bar = 28µm); (c) Control A549 cell cultures at 24 hr: focal ß-catenin expression on the plasma membrane at intercellular contacts (arrows) and irregular cytoplasmic expression (arrows) (bar = 28µm); (d) FE-treated A549 cell cultures at 24 hr: β-catenin expression (arrows) is increased compared with control A549 cells (c), (bar = 28µm); (e) Control A549 cells at 48 hr: moderate expression of VEGF mainly at the perinuclear level (arrows), (bar = 12µm); (f) FE-treated A549 cells at 48 hr: VEGF expression (arrows) is similar to A549 control cultures (e), (bar = 14µm); (g) Control A549 cells at 48 hr: ß-catenin expression (arrows) is evident on the cell membrane and faint in cytoplasm (bar = 14µm); (h) FE-exposed A549 cells at 48 hr: β-catenin positivity (arrows) is similar to that noted in control cultures (g) even though it is less faint in the cytoplasm (bar = 12µm).

VEGF and ß-catenin expression in control and FE-treated MeT-5A cells at 24 and 48 hr (Fig. 7; Tab. 1).

At 24 hr, FE-treated MeT-5A cells showed a higher expression of both VEGF and ß-catenin in the cytoplasm and plasma membrane compared with controls, whereas at 48 hr they displayed an increased number of cells staining for the two markers and a more intense expression of both molecules (greater for ß-catenin) only in the cytoplasmic compartment.

24 hr (Fig. 7 a-d). Control cells displayed modest perinuclear and peripheral cytoplasmic VEGF expression, (Fig. 7 a), while treated cells exhibited stronger VEGF expression (Fig. 7 b). In control cultures ß-catenin expression (Fig. 7 c) was both in the cytoplasm and in the plasma membrane; staining was evident in treated cells, especially in the cytoplasm (Fig.7 d).

48 hr (Fig. 7 e-h). Moderate VEGF expression (Fig. 7 e), mainly in the perinuclear cytoplasm, was detected in control cells. FE-exposed cells displayed more intense VEGF positivity, again in the perinuclear zone (Fig. 7 f), and a significantly greater number of positive cells compared with control cultures (p= 0.005).

In control cultures expression of ß-catenin was irregular and mainly at membrane junctions (Fig. 7 g), whereas it was slightly stronger in treated cells, above all in the cytoplasm (Fig. 7 h); positive cells were significantly more numerous in treated than in control cultures.

Western blot analysis and PGE$_2$ determination

Finally, we used mouse monocyte-macrophage J774 cells to investigate the effects of FE exposure on the time course of *in vitro* generation of PG biosynthesis and on the gene expression and protein synthesis of a key enzyme in the inflammatory process, inducible COX-2 (COX-2: Figure 8; PGE$_2$: Figure 9). As expected, COX-2 and PGE$_2$ levels were low in control cultures; FE exposure for 24 hr and 48 hr induced a significant and time-dependent increase, as shown by the fact that synthesis of COX-2 and PGE$_2$ rose respectively by 23% and 2.8% at 24 hr and by 8.5% and 5.1% at 48 hr compared with control cells.

DISCUSSION

The recent recognition of fluoro-edenite as a new edenite end-member its association with the abnormal incidence of pleural mesothelioma

recorded among the residents of Biancavilla (16, 18, 33) mandates further study of the amphibole, especially of the salient aspects of its toxicity and its role in neoplastic cell transformation. The present investigation was conducted on cell systems widely employed in the evaluation of mineral fibre cytotoxicity to clarify the mechanisms involved in mesothelioma development among the population of Biancavilla.

It is well established that a) there is a functional relationship between inflammation and cancer and that b) cancer frequently arises in areas of chronic inflammation (28).

Moreover, lung epithelial and mesothelial cells are also known to be directly involved in inflammatory cross-talks via production of growth factors and redistribution of cytoskeletal molecules, that affect intercellular relationships in tissues (6, 8, 9).

Our data are in line with epidemiological analyses and *in vitro* short-term dose-response studies showing the critical importance of epithelial and mesothelial cross-talks in lung conditions due to mineral fibre exposure. Results show differential alteration of cytoplasmic F-actin networks, cell motility and VEGF and β-catenin expression in treated A549 and MeT-5A cells, according to the different sensitivity of the two cell lines. Treated J774 cells exhibited a significantly increased expression of COX-2 and PGE$_2$ concentrations.

The altered distribution of F-actin and impaired cell motility after fibre exposure demonstrate that FE toxicity affects cell motility (7) and point to parallel functional modifications in MeT-5A and A549 cells, despite their different sensitivities.

Time-lapse videomicroscopy analyses, conducted to gain insights into the correlation between fluorescence data and cell movement, showed that MeT-5A cell motion stopped almost completely after 24 hr exposure to FE. In addition, the "granular" appearance of actin fluorescence indicates impaired actin polymerization in presence of the fibres. Thus, time-lapse and fluorescence findings concur in demonstrating a cytoskeletal impairment after 24 hr exposure, followed by evident cell damage at 48 hr. The pathogenicity of FE fibres is indicated by the almost total arrest of cell movement at 48 hr in both cell lines as well as by the "flocculation" of fluorescent F-actin molecules.

At 24 hr, VEGF expression was significantly increased in A549 cells (p<0.05),
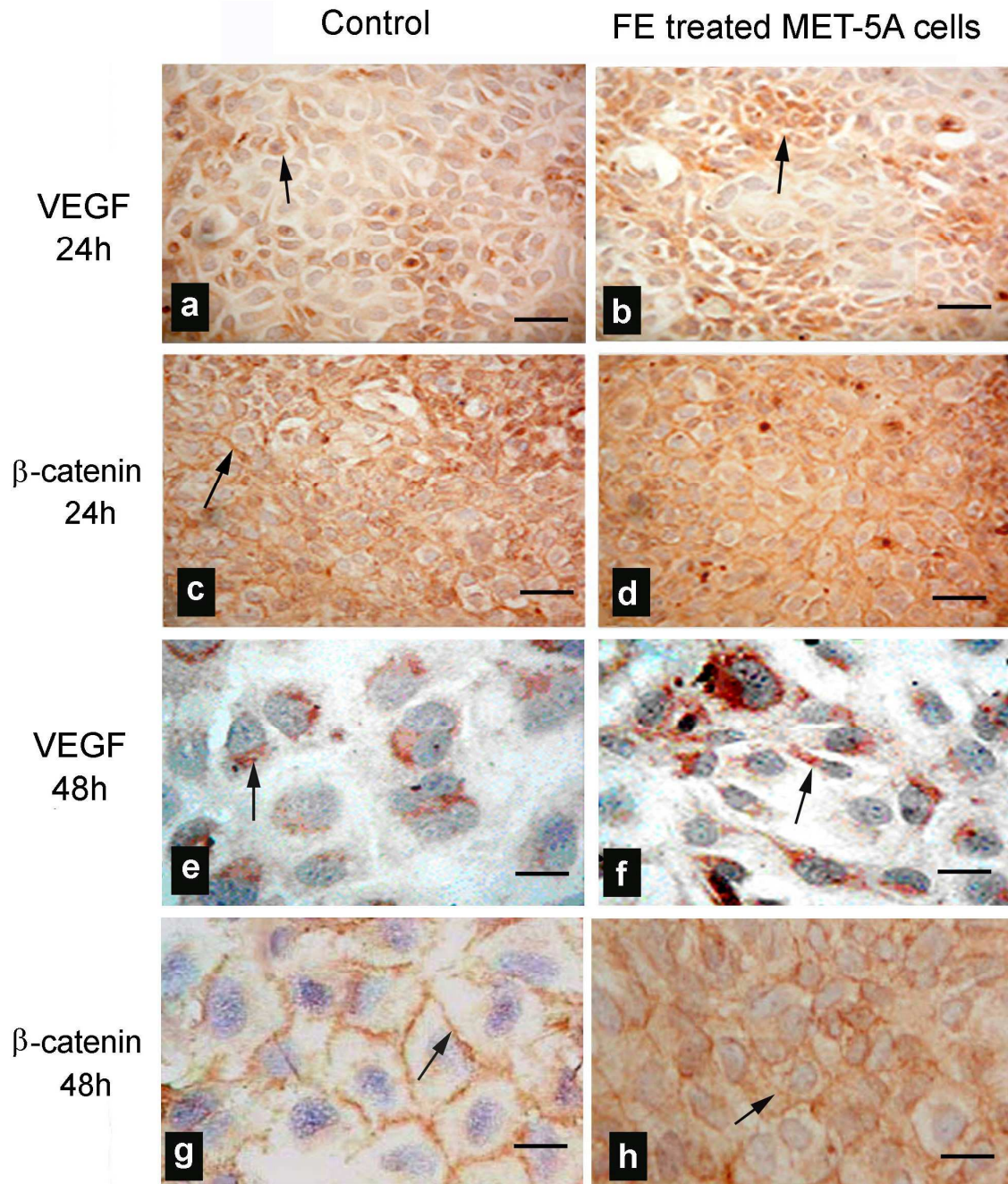
Figure 7 (a-h). VEGF and ß-catenin expression in control and FE-treated MeT-5A cell cultures at 24 (a-d) and 48 hr (e-h), (immunoperoxidase). (a) Control MeT-5A cells at 24 hr: modest VEGF expression (arrows) both in the perinuclear zone and in cytoplasmic extensions (bar = 28µm); (b) FE-treated MeT-5A cells at 24 hr: treated cells exhibited higher VEGF expression (arrows) than control cultures (a), (bar = 28µm); (c) Control MeT-5A cells at 24 hr: ß-catenin (arrows) is expressed both in cytoplasm and in the plasma membrane (bar = 21µm); (d) FE-treated MeT-5A cells at 24 hr: evident ß-catenin staining, especially in cytoplasm, compared with control cells (c) (bar = 21µm); (e) control MeT-5A cells at 48 hr: moderate VEGF expression (arrows), principally in perinuclear cytoplasm (bar = 10µm); (f) FE-treated MeT-5A cells at 48 hr: positivity for VEGF (arrows) is stronger than in control cells (e) (bar = 12µm); (g) Control Met-5A cells at 48 hr: irregular β-catenin expression (arrows), mainly at membrane-junctional levels (bar = 12µm); (h) FE-treated MeT-5A cells at 48 hr: slightly stronger β-catenin expression (arrows), mainly in the cytoplasm, compared with control cells (g), (bar = 14µm).
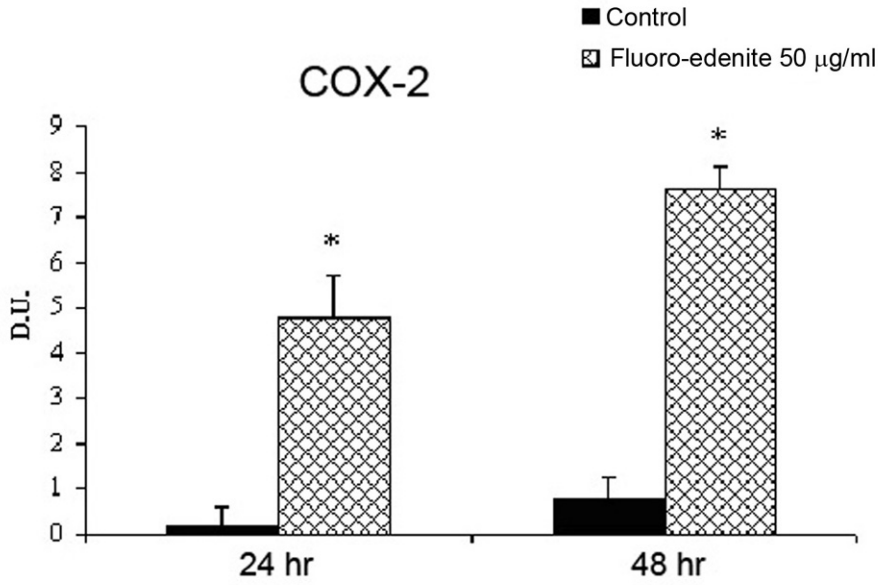
Figure 8. COX-2 expression evaluated by Western blot analysis in untreated and FE-treated monocyte-macrophage J774 cells. COX-2 levels are expressed as Densitometric Units (DU). Each value is the average of four different experiments $\pm$ SD. Statistics: *significant vs untreated control (P<0.01).
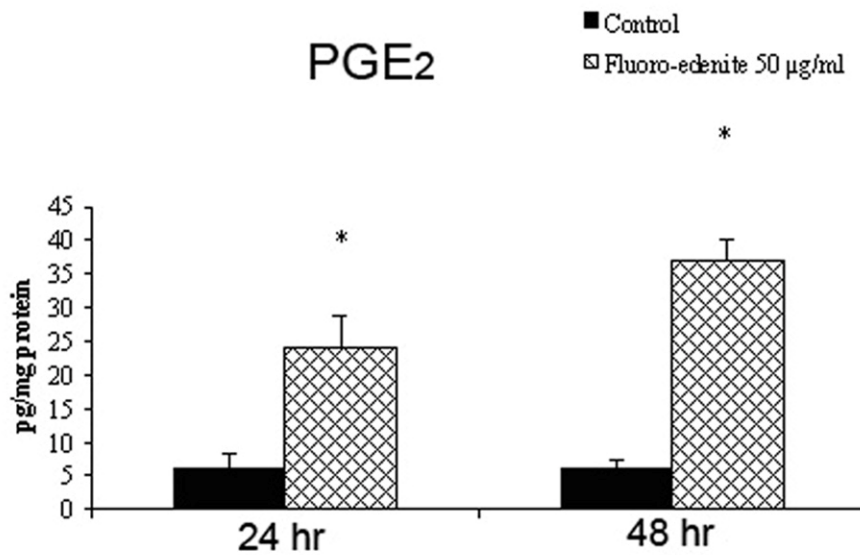
Figure 9. Concentration of PGE_2 measured in the culture media by ELISA in untreated and FE-treated monocyte-macrophage J774 cells. Each experiment was performed three times in duplicate. Statistics: *significant vs untreated control (P<0.01).

whereas MeT-5A cells exhibited a marked increase in molecular expression that was greater for β-catenin (p<0.05). Both molecules are known to be involved in cancer development (10, 35).

After 48 hr incubation, VEGF and ß-catenin activity were still evident in both cell lines, suggesting that at concentrations comparable to those tested for other toxic mineral fibres, such as chrysotile (25), FE fibres do not exert a primary toxic action inducing rapid cell death, but rather induce an abnormal cellular status with upregulated cell activities and a risk of cell transformation.

These data lend support to the hypothesis that FE is capable of triggering *in vivo* cell transformation mechanisms also through upregulation of the Wnt-ß-catenin signal transduction pathway and VEGF synthesis (3, 10, 35).

Previous studies of FE-exposed human lung fibroblasts, the human lung alveolar epithelial cancer cell line A549 and the monocyte-macrophage cell line J774 by our group evidenced a concentration- and time-dependent reduction in cell metabolism and increased LDH release, concomitant with an increase in ROS production and DNA damage (8,9). In addition, Travaglione et al. (33) noted a remarkable tropism of A549 cells towards FE fibres, which interfered with epithelial cell physiology by reducing proliferation rate and increasing release of the proinflammatory cytokine IL-6, one of the main mediators of asbestos-induced pathophysiological responses.

In this investigation we demonstrated time-dependent COX-2 overexpression and PGE$_2$ increase in monocyte-macrophage J744 cells treated with FE using Western blotting and ELISA. COX-2 is an inducible enzyme with a central role in the conversion of arachidonic acid to a number of metabolites including prostaglandins. Its activity is low in normal conditions, but increases in macrophages, fibroblasts, vascular endothelial cells, neurons and other tissues in response to various stimuli, including cytokines, carcinogens, serum, hormones, and mitogens, and participates in inflammation and cell proliferation and differentiation processes (20, 23). Furthermore, COX-2 expression is upregulated in a variety of malignancies, including breast, gastric, oesophageal and lung cancer, hepatocellular carcinoma, squamous cell carcinoma of head and neck and pancreatic cancer (34). PGE$_2$ derived from COX-2 is involved in solid tumour pathogenesis through inhibition of apoptosis, facilitation of tumour cell invasiveness and promotion of angiogenesis.

Our studies clearly demonstrate a role for oxidative stress, COX-2 activity and inflammatory factors in the development and progression of mesothelioma induced by FE.

Several findings indicate that inflammation has both negative and positive aspects; a number of questions concerning dysregulation of inflammatory processes thus arise when mediators of inflammation injury or repair are considered. In our study, the role of macrophage cytokine expression after *in vitro* exposure to FE has been considered in parallel with direct fibre toxicity in lung alveolar epithelial and mesothelial cell lines. Toxicity responsiveness in established lung cell lines has already been documented to further contribute to abnormal cell changes also through altered cytokine responses (IL-6, TNFα, etc.), and shows how A549 cells develop a response to inflammatory stimuli (30). Our data confirm these effects of FE fibres when A549, MeT-5A and J774 cells are exposed to a fibre concentration of 50 μg/ml, and further stress the close relationship between toxicity and the inflammatory response induced by the toxic effects of FE.

We employed natural fibres directly collected from a stone quarry on M. Calvario, near Biancavilla. Their characterization using SEM-EDS showed the presence of edenite and fluoro-edenite-like fibres, whose respective percent composition was impossible to quantify since their relative amount varied among bundles and even in contiguous areas. Both are respirable fibres capable of being carried by the circulation, having been found in lung (human and sheep) and in other biological samples (urine) from people living in Biancavilla (2).

In conclusion, we provide convincing evidence that FE fibres are capable of inducing *in vitro* functional modifications of some parameters that are closely involved in the development and progression of cancer. The present findings suggest that inhaled FE fibres are capable of inducing mesothelioma, even though their ability to penetrate into the lung alveoli closely depends on their aerodynamic diameter.

REFERENCES

1. Balkwill, F., Mantovani, A., Inflammation and cancer: back to Virchow? *Lancet* 2001, **357**: 539-545.

2. Battaglia, T., Belluso, E., Capella, S., Fornero, E., Ferraris, G., Bellis, D., Biagini, G., Pugnaloni, A., Panico, A.M., Cardile, V,. European Conference, "Asbestos Monitoring and Analytical Methods", 5-7 Dec 2005, Auditorium Santa Margherita, Venezia, Italy.

3. Beachy, PA., Karhadkar, SS., Berman, DM., Tissue repair and stem cell renewal in carcinogenesis. *Nature* 2004, **432**: 324-331.

4. Bergamini, C., Fato, R., Biagini, G., Pugnaloni, A., Giantomassi, F., Foresti, E., Lesci, GI., Roveri, N., Lenaz, G., Mitochondrial changes induced by natural and synthetic asbestos fibres. Studies on isolated mitochondria. *Cell Mol Biol* 2004, **50**: 691-700.

5. Bhowmick, NA., Neilson, EG., Moses, HL., Stromal fibroblasts in cancer initiation and progression. *Nature* 2004, **432**: 332-37.

6. Blanco, D., Vincet, S., Elizegi, E., Pino, I., Fraga, MF., Esteller, M., Saffiotti, U., Locanda, F., Montuenga, LM., Altered expression of adhesion molecules and epithelial–mesenchymal transition in silica induced rat lung carcinogenesis. *Lab Invest* 2004, **84**: 999-1012.

7. Boardman, KC., Aryal, AM., Miller, WM., Waters, CM., Actin redistribution in response to hydrogen peroxide in airway epithelial cells. *Cell Physiol* 2004, **199**: 57-66.

8. Cardile, V., Proietti, L., Panico, AM., Lombardo, L.,. Nitric oxide production in fluoro-edenite treated mouse monocyte-macrophage cultures. *Oncol Reports* 2004a, **12**: 1209-1215.

9. Cardile, V., Renis, M., Scifo, C., Lombardo, L., Gulino, R., Mancari, B., Panico, AM., Behaviour of the new asbestos amphibole fluoro-edenite in different lung cell systems. *IJBCB* 2004b, **36:** 849-860.

10. Chen, S., Guttridge, DC., You, Z., Zhang, Z., Fribley, A., Mayo, MW., Kitajewski, J., Wang, CY., Wnt-1 Signaling inhibits apoptosis by activating Bcatenin/T cell Factor–mediated transcription. *J Cell Biol* 2001, **152**: 87-96.

11. Comba, P., Gianfagna, A., Paoletti, L., Pleural mesothelioma cases in Biancavilla are related to a new fluoro-edenite fibrous amphibole. *Arch Environ Health* 2003, **58**: 229-32.

12. Derbyshire E., Natural aerosolic mineral dusts and human health. In: *Essentials of medical geology* Selinus O, Alloway B, Centeno JA, Finkelman RB, Fuge R, Lindh U, Smedley P (Eds), Burlington, San Diego, London, Elsevier Academic Press, 2005, pp.459-480.

13. De Witt, D.L., Prostaglandin endoperoxide synthase: regulation of enzyme expression. *Biochim Biophys Acta* 1991, **60:** 121-134.

14. Fenoglio, I., Croce, A., Di Renzo, F., Tiozzo, R., Fubini, B., 2000. Pure-silica zeolites (Porosils) as model solids for the evaluation of the physicochemical features determining silica toxicity to macrophages. *Cement Res Toxicol* **13**: 489-500.

15. Gazzano, E., Riganti, C., Tomatis, M., Turci, F., Bosia, A., Fubini, B., Ghigo, D., Potential toxicity of nonregulated asbestiform minerals: balangeroite from the western Alps. Part 3: Depletion of antioxidant defenses. *J Toxicol Environ Health A.* 2005, **8**: 41-9.

16. Gianfagna, A., Oberti, R., Fluoro-edenite from Biancavilla (Catania, Sicily, Italy): Crystal chemistry of a new amphibole end-member. *Am Mineral* 2001, **86**: 1489-1493.

17. Godleski, JJ., Role of asbestos in etiology of malignant pleural mesothelioma. *Thorac Surg Clin* 2004, **14**: 479-487.

18. Grice, JD., Ferraris, G., New minerals approved in 2000 by the Commission on New Minerals and Mineral Names . IMA (No 2000-a49,p.1001). *Eur J Mineral* 2000, **13**: 995-1002.

19. Guilianelli, C., Baeza-Squiban, A., Boisvieux-Ulrich, E., Houcine, O., Zalma, R., Guennou, C., Pezerat, H., Marano, F. Effect of mineral particles containing iron on primary cultures of rabbit tracheal epithelial cells: possible implication of oxidative stress. *Environ Health Persp* 1993, **101**: 436-442.

20. Hla, T., Neilson, K., Human cyclooxygenase-2 cDNA. *Proc Natl Acad Sci USA* 1992, **89:** 7384-7389.

21. Holian, A., Kelley, K., Hamilton, R.F. Jr.,. Mechanisms associated with human alveolar macrophage stimulation by particulates. *Environm Health Persp* 1994, **102**: 69-74.

22. Laemnli, U.K., Cleavage of structural proteins during the assembly of the head of bacteriophage T4. *Nature* 1970, **277**: 680-685.

23. Lee, S.H., Soyoola, E., Chanmugan, P., Hart, S., Sun, W., Zhong, H., Liou, S., Simmons, D., Hwang, D., Selective expression of mitogen-inducible cyclooxygenase in macrophage stimulated with lipopolysaccharide. *J Biol Chem* 1992, **26**: 25934-25938.

24. Levresse, V., Renier, A., Levy, F., Broaddus, V.C., Jaurand, M. DNA breakage in asbestos-treated normal and transformed (TSV40) rat pleural mesothelial cells. *Mutagenesis* 2000, **15**: 239-244.

25. Lindroos, PM., Coin, PG., Badgett, A., Morgan, DL., Bonner, JG., Alveolar macrophages stimulated with titanium dioxide, chrysotile asbestos, and residual oil fly ash upregulate the PDGF receptor-alpha on lung fibroblasts through an IL-1 beta-dependent mechanism. *Am J Respir Cell Biol* 1997, **16**: 283-292.

26. Paoletti, L., Batisti, D., Bruno, C., Di Paola, M., Gianfagna, A., Mastrantonio, M., Nesti, M., Comba, P. Unusually high incidence of malignant pleural mesothelioma in a town of eastern Sicily: an epidemiological and environmental study. *Arch Environ Health* 2000, **55**: 392-8.

27. Pasetto R., Bruni B., Bruno C., D'Antona C., De Nardo P., Di Maria G., Di Stefano R., Fiorentini C., Gianfagna A., Marconi A., Paletti L., Putzu MG., Soffritti M., Comba P. Problematiche sanitarie della fibra anfibolica di Biancavilla. Aspetti epidemiologici, clinici e sperimentali. *Not Ist Super Sanità* 2004, **17**: 8-12.

28. Pikarsky, E., Porat, RM., Stein, I., Abramovitch, R., Admit, S., Kasem, S., Gutkovich-Pyest, E., Urieli-Shoval, S., Galum, E., Ben-Neriah, Y., NFKappaB Function as a tumor promoter in inflammation –associated cancer. *Nature* 2004, **431**: 461-466.

29. Puhakka, A., Ollikainen, T., Soini, Y., Kahlos K., Säily Pirjo Koistinen, M., Pääkkö, P., Linnainmaa, K., L. Kinnula V., Modulation of DNA single-strand breaks by intracellular glutathione in human lung cells exposed to asbestos fibers. *Mutat Res* 2002, **514**: 7-17.

30. Ramage, L., Proudfoot, L., Guy, K. Expression of C-reactive protein in human lung epithelial cells and upregulation by cytokines and carbon particles. *Inhal Toxicol* 2004, **16**: 607-13.

31. Scalise, A., Tucci, MG., Lucarini, G., Giantomassi, F., Orlando, F., Pierangeli, M., Pugnaloni, A., Bertani, A., Ricotti, G., Biagini, G., Local rh-VEGF administration enhances skin flap survival more than other types of rh-VEGF administration: a clinical, morphological and immunohistochemical study. *Exp Dermatol* 2004, **13**: 682-690.

32. Shukla, A., Gulumian, M., Hei, T.K., Kamp, D., Rahman, Q., Mossman, B., Multiple roles of oxidants in the pathogenesis of asbestos-induced diseases. *Free Radical Biol Med* 2003, **3**: 1117-1129.

33. Travaglione, S., Bruni, B., Falzano, L., Paoletti, L., Fiorentini, C., Effects of the new –identified amphibole FE in lung epithelial cells. *Tox Vit* 2003, **17**: 547-552.

34. Williams, C., Shattuck-Brandt, R.L., Dubois, R.N.,. The role of COX-2 in intestinal cancer. *Expert Opin Investig Drugs* 1999, **8:** 1-12.

35. Zheng R., Yano S., Matsumori Y., Nakataki E., Muguruma H., Yoshizumi M., Sone S., SRC tyrosine kinase inhibitor, m475271, suppresses subcutaneous growth and production of lung metastasis via inhibition of proliferation, invasion, and vascularization of human lung adenocarcinoma cells. *Clin Exp Metastasis* 2005, **22**: 195-204.